Dynamos with a flat α-effect distribution

A. Brandenburg , I. Tuominen & F. Krause

DYNAMOS WITH A FLAT α-EFFECT DISTRIBUTION

A. BRANDENBURG and I. TUOMINEN

*Observatory and Astrophysics Laboratory, University of Helsinki, Tähtitorninmäki,
SF-00130 Helsinki, Finland*

F. KRAUSE

*Sternwarte Babelsberg, Akademie der Wissenschaften der DDR,
Rosa-Luxemburg-Str. 17a, 1591 Potsdam, German Democratic Republic*

In order to obtain a better insight into the excitation conditions of magnetic fields in flat objects, such as galaxies, we have calculated critical dynamo numbers of different magnetic field modes for spherical dynamos with a flat α-effect distribution. A simple but realistic approximation formula for the rotation curve is employed. In most cases investigated a stationary quadrupole-type solution is preferred. This is a consequence of the flat distribution of the α-effect. Non-axisymmetric fields are in all cases harder to excite than axisymmetric ones. This seems to be the case particularly for flat objects in combination with a realistic rotation curve for galaxies. The question of whether non-axisymmetric (bisymmetric) fields, which are observed in some galaxies, can be explained as dynamos generated by an axisymmetric αω-effect is therefore still open.

KEY WORDS: α-effect, dynamo action, galactic dynamos.

1. INTRODUCTION

Whether or not a magnetic field in a cosmical object can be explained by a dynamo depends on the excitation conditions of the competing magnetic field modes of different symmetry type: in a sufficiently weak nonlinear regime only that mode which can be excited most easily is of physical interest (Krause and Meinel, 1988). However, it is necessary to investigate the distribution of the marginal dynamo numbers in parameter space also for some of the other modes. Only then is it possible to discuss the tendencies that the object has towards different types of solutions under various circumstances.

   The calculation of a complete set of eigenvalues is a solved problem for spherical objects. However, for flat objects, e.g. galactic disks, the solutions so far presented have been obtained under certain approximations which are derived from plane layer models (Zeldovich *et al.*, 1983; see also Baryshnikova *et al.*, 1987). One cannot be sure that the eigenvalues of these models are representative for disks with a finite radial extension (Krause, 1990).

The results we present here are based on methods similar to those we used earlier for the investigation of spherical dynamo models (see Brandenburg *et al.*, 1989b). The step towards flat objects is achieved following the concept of Elstner *et al.* (1990). We assume flat profiles for the α-effect embedded in a homogeneously conducting sphere which may emulate a galactic halo. The assumption of constant magnetic diffusivity, η, in the halo is made for the sake of simplicity. However, investigations of models with a flat distribution of η have shown that the excitation conditions between different modes can be changed substantially (see Donner and Brandenburg, 1990).

Our main interest is the question of whether there are conditions under which non-axisymmetric fields can be more easily excited than axisymmetric ones. For reasons of convergence it is clear that our method can hardly apply to objects with realistic flatness; only the tendencies can be studied here. In order to gain deeper insight more appropriate methods have to be developed (cf. Elstner *et al.*, 1990; Moss and Tuominen, 1990).

2. BASIC EQUATIONS AND MODELS

We consider dynamo action in a rotating and conducting sphere of radius R surrounded by empty space. The generation of a mean magnetic field, **B**, can be described by the induction equation

$$\frac{\partial B}{\partial t} = \nabla \times (\mathbf{u} \times \mathbf{B} + \mathscr{E} - \eta \nabla \times \mathbf{B}), \tag{1}$$

which applies inside the sphere. We assume that the electric current vanishes outside the sphere, which implies that the field continues as a potential field outside; η is the magnetic diffusivity of the fluid, which is considered to be constant; **u** is the velocity of the mean motion of the fluid and $\mathscr{E}$ is the mean electromotive force caused by fluctuations of the motions and of the magnetic field. For $\mathscr{E}$ we take here only the usual α-effect

$$\mathscr{E} = \alpha \mathbf{B}, \tag{2}$$

where α depends on the spatial coordinates. For the mean motion we assume only a differential rotation given by:

$$\mathbf{u} = \mathbf{\Omega} \times \mathbf{r}, \tag{3}$$

where $\mathbf{\Omega}$ is the mean angular velocity.

2.1. The Numerical Method

The equations governing the **B**-field pose an eigenvalue problem for the complex eigenvalue λ, where $\mathcal{R}e\,\lambda$ is the growth rate and $\mathcal{I}m\,\lambda$ the eigenfrequency. We look for marginal dynamo numbers C_α (see later), for which the largest growth rate vanishes. We represent **B** in terms of poloidal and toroidal field parts by

$$\mathbf{B} = \nabla \times \nabla \times (\hat{\mathbf{r}}S) + \nabla \times (\hat{\mathbf{r}}T) \tag{4}$$

and expand the functions S and T as a series of spherical harmonics. We then obtain an eigenvalue problem for an infinite set of ordinary differential equations for S_l^m and T_l^m. This is solved numerically using a truncated set of equations with N_l spherical harmonics and N_r grid points in the radial direction. We usually solve first *all* eigenvalues to relatively low accuracy, by adopting small truncation parameters N_r and N_l. After this we increase the truncation parameters and then look only for the eigenvalue with the largest growth rate, $\mathcal{R}e\,\lambda$. For further details see Brandenburg *et al.* (1989b).

2.2. The α-distribution

We are interested in an α-distribution which changes sign at the equator and which approaches zero at some relative height z_0 above and below the equatorial plane. A simple expression is:

$$\alpha = \alpha_0 \begin{cases} z(z_0^2 - z^2), & \text{if } |z| \leqq z_0, \\ 0, & \text{if } |z| \geqq z_0, \end{cases} \tag{5}$$

where z is the coordinate in the direction parallel to the rotation axis normalized by R. Here we have introduced a constant α_0 which is related to the dynamo number $C_\alpha = \alpha_0 R/\eta$. We express α in spherical coordinates (i.e. $z = r\cos\theta$, r being the relative distance from the center) and expand it in terms of Legendre polynomials:

$$\alpha(r, \theta) = \sum_{l=1,3,\ldots}^{N} \alpha_l(r) P_l(\cos\theta), \tag{6}$$

where N_α is a truncation level of this expansion. The functions $\alpha_l(r)$ can be calculated from

$$\alpha_l(r) = \tfrac{1}{2}(2l+1) \int_{-1}^{1} d(\cos\theta)\alpha(r,\theta)P_l(\cos\theta). \tag{7}$$

The analytic expressions for the first terms are given in Table 1. In the upper row of Figure 1 the functions $\alpha_l(r)$ for different values of l between 1 and 7 have been

Table 1 The results for the functions $\alpha_l(r)$ for $l = 1, 3, 5$, and 7. We have used $\zeta \equiv z_0/r$ as an abbreviation and α_l has been normalized here to α_0.

	$r \leqq z_0$	$r > z_0$
α	$\alpha_1 \frac{1}{5} r^3 [5\zeta^2 - 3]$	$\frac{2}{5} r^3 \zeta^5$
α_3	$-\frac{2}{5} r^3$	$\frac{1}{5} r^3 \zeta^5 [5\zeta^2 - 7]$
α_5	0	$\frac{11}{4} r^3 \zeta^5 [\zeta^4 - 2\zeta^2 + 1]$
α_7	0	$\frac{5}{8} r^3 \zeta^5 [13\zeta^6 - 33\zeta^4 + 27\zeta^2 - 7]$

plotted. Note that the alternating positive and negative contributions from the terms α_l are of nearly equal size. This would suggest that the expansion does not converge very quickly. The shape of the α-profile for retaining only the first few modes can be seen in the lower row of Figure 1. We feel that the last case with $N_\alpha = 7$ resembles sufficiently well a flat distribution of α. The relative thickness used in Figure 1 was $z_0 = 0.3$. For thinner disks one should take more terms into account.

For the rotation velocity $v \equiv u_\phi(r, \pi/2)$ we take here a simple empirical formula:

$$v = v_0 r \left[1 + \left(\frac{r}{r_0} \right)^n \right]^{-1/n}, \qquad (8)$$

where r_0 is the characteristic radius at which the solid body rotation close to the center changes to a constant velocity. The parameter n determines how sharp this transition is. The strength of the rotation is measured by a non-dimensional number $C_\omega = v_0 R/\eta$. The functions $v(r)$ and $\Omega(r) = v/r$ have been plotted in Figure 2 together with the rotational shear $\partial\Omega/\partial r$ which determines the local production of the toroidal field from the poloidal field. Note that the angular velocity here is constant on concentric shells. We feel that this assumption is reasonable, because the magnetic field close to the axis of rotation and far away from the disk turns out to be quite weak and is therefore not much influenced by Ω. In Figure 2 we have used the values $r_0 = 0.2$ and $r_0 = 0.5$ on the left-hand and on the right-hand side, respectively. For the parameter n we have always taken $n = 2$, which is typical of the observed rotation curves for galaxies (see for example Ruzmaikin *et al.*, 1988).

3. RESULTS AND DISCUSSION

For all the models presented here we have chosen for the truncation level in the expansion of α [see (6)] the value $N_\alpha = 7$. We consider first the case with $z_0 = 0.3$ and $r_0 = 0.5$. Then we study models with different values of z_0 and r_0. A summary showing the dependence of the marginal dynamo numbers on C_ω is given in Figure 3.
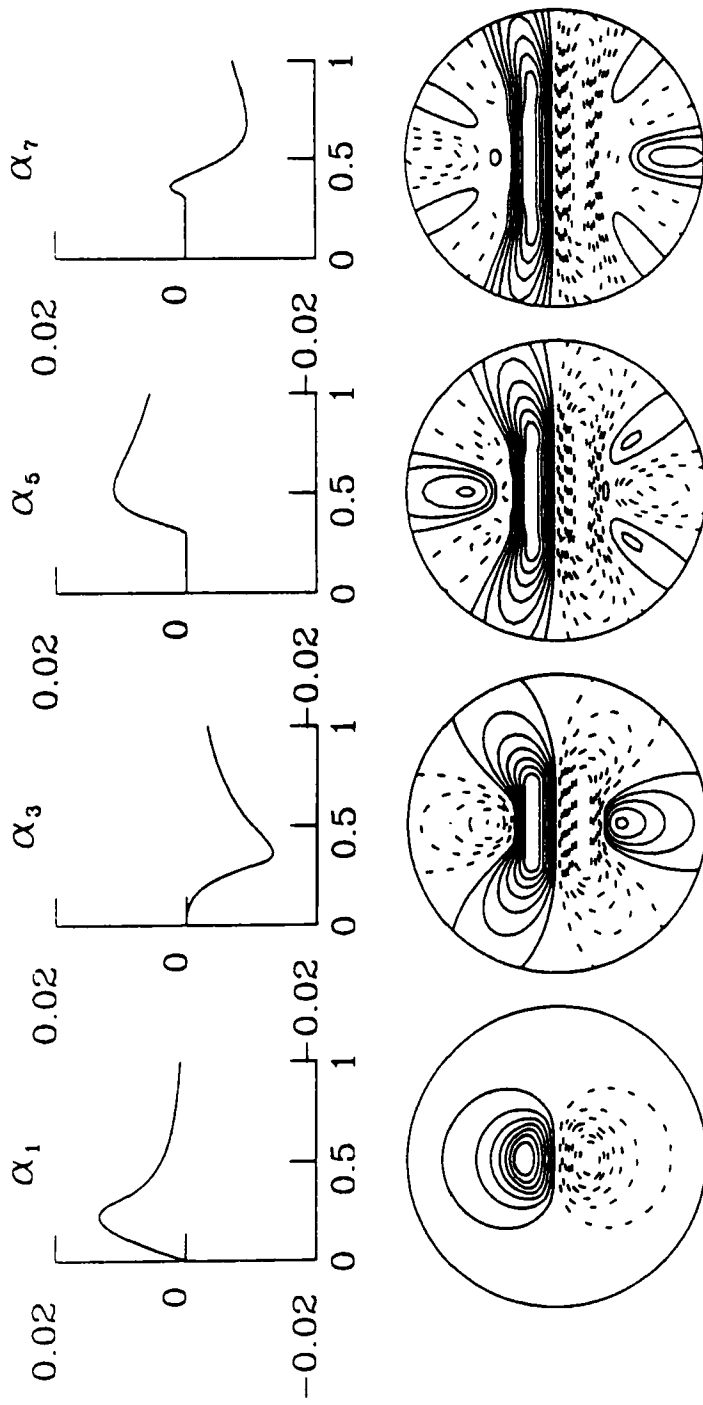
Figure 1 In the upper row the first non-vanishing coefficients α_i from the expansion of Eq. (7) are plotted for $z_0 = 0.3$. In the second row the α-distribution is shown taking only the first few terms in the α expansion into account. The left-most panel is for the case with $N_\alpha = 7$, which was used for all computations of this paper; α is normalized here to α_0. Dotted contours refer to a negative value.
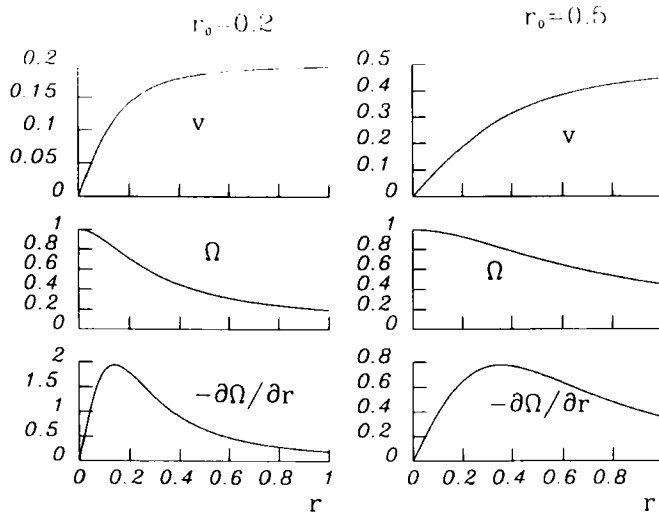
Figure 2 The functions $v(r)$, $\Omega = v/r$ and $\partial\Omega/\partial r$ for the values $r_0 = 0.2$ and $r_0 = 0.5$, respectively. (Here v has been normalized with v_0.)
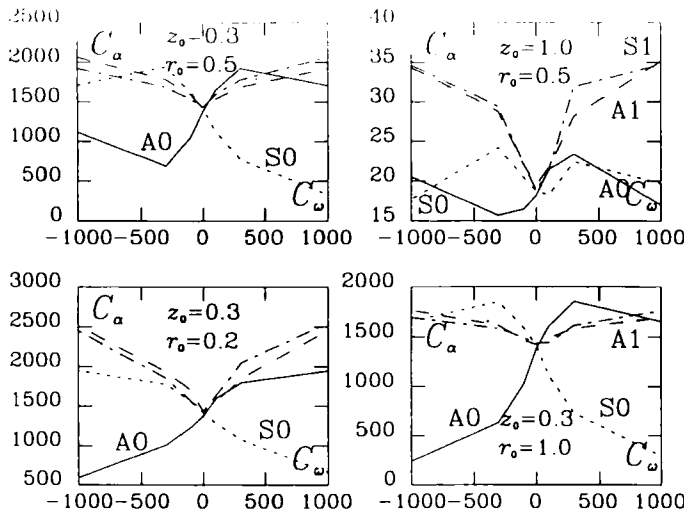

Figure 3 Summary of four different models considered. The marginal dynamo number C_α has been plotted versus C_ω for the modes $A0$ (solid), $S0$ (broken), $A1$ (dashed), and $S1$ (dot-dash). The values for z_0 and r_0 have been marked inside each panel. Note in particular the different behavior of the $A0$- and $S0$-mode between the cases with $z_0 = 0.3$ (top left) and $z_0 = 1.0$ (top right) for $|C_\omega| = 1000$.

3.1 Models with Different Disk Thickness z_0

The results for the marginal dynamo number, C_α, and the eigenfrequency, $\mathcal{I}m\,\lambda$, are given in Table 2 for different strengths of differential rotation (measured by

Table 2 Marginal dynamo numbers for a model with $z_0 = 0.3$ and $r_0 = 0.5$. max $(\alpha) = 1.06 \times 10^{-2}$. The smallest value of C_α for a given value of C_ω is printed in bold face. The truncation level is $N_r = 50$ and $N_l = 10$.

C_ω	$A0$	$S0$	$A1$	$S1$
-1000	**1120**	1707	2063	1919
-300	**687**	1943	1779	1686
-100	**1057**	1624	1594	1536
0	**1386**	1412	1420	1436
100	1643	**1131**	1535	1590
300	1925	**768**	1686	1778
1000	1706	**327**	1922	2065
		$-\mathscr{I}m\,\lambda$		
-1000	0	± 95.8	-917	-910
-300	0	± 10.7	-262	-259
-100	0	0	-80	-80
0	0	0	-0.57	$+0.57$
100	0	0	80	79
300	± 11.7	0	259	261
1000	± 96	0	909	917

C_ω). For $C_\omega = 0$ the $A0$-mode has the smallest critical dynamo number and is therefore the easiest to excite. (The smallest value C_α for a given $C_\omega = 0$ has been printed in bold face.) For positive values of C_ω (< 1000) the $S0$-mode is preferred. In contrast, for negative values of C_ω the $A0$-mode is preferred. This finding is in agreement with the results for ellipsoids obtained by Stix (1975). On the other hand, it is well known that for most of the dynamo models for the Sun or planets the $A0$-mode has the smallest critical dynamo model number when α is positive and $\partial\Omega/\partial r$ negative, i.e. $C_\alpha > 0$ and $C_\omega > 0$ (see e.g. Roberts and Stix, 1972; Rädler, 1986; see also the stability map in Figure 1 by Brandenburg et al., 1989a).

In order to see whether this is a consequence of the flat α-effect distribution, we have presented in Table 3 the results for the same model but with $z_0 = 1$. Note at first that all values of $C_\alpha > 0$ are two orders of magnitude smaller than in the previous case. The basic reason for this is that the maximum of α is in this case much larger (0.39, while it was 0.011 in the previous case). More important is that for $|C_\omega| = 1000$ the preference of the $A0$- and $S0$-modes is reversed compared with the previous model, i.e. for $C_\alpha > 0$ and $C_\omega > 0$ the $A0$-mode is the easiest to excite. This result confirms that this property is really due to the flat α-effect distribution. The non-axisymmetric modes are, in the presence of differential rotation, in both cases much harder to excite. Only for $C_\omega = 0$ are the marginal values of C_α, for all the modes, very close together (Rädler, 1986a).

Although the vertical extension of the *ionized* gas in the galactic halo is uncertain, it seems that the thickness of the α-effect distribution in the first case is, with $z_0 = 0.3$, still far too large to resemble real galaxies. Therefore in the next model we decreased the thickness by a factor of three, i.e. we set $z_0 = 0.1$, keeping

Table 3 Marginal dynamo numbers for the same model as in Table 2, but with $z_0 = 1.0$, $\max(\alpha) = 0.39$.

C_ω	$A0$	$S0$	$A1$	$S1$
-1000	20.5	**17.7**	34.3	34.6
-300	**15.7**	24.2	28.8	29.4
-100	**16.5**	20.4	22.0	22.1
0	**18.2**	18.7	19.5	18.8
100	21.4	**18.2**	21.7	21.3
300	23.4	**22.4**	28.2	31.9
1000	**17.0**	19.7	35.1	34.7
		$-\mathscr{I}m\,\lambda$		
-1000	± 36.7	± 39.8	-480	-478
-300	0	± 13.6	-154	-152
-100	0	0	-59.4	-60.3
0	0	0	0.49	1.94
100	0	0	62.7	62.6
300	± 15.1	± 8.3	186	173
1000	± 39.0	± 36.1	478	48.1

Table 4 Marginal dynamo numbers, divided by 10^3, for the same model as in Table 2, but for a thinner disk with $z_0 = 0.1$, $\max(\alpha) = 3.9 \times 10^{-4}$. The results are not all of the same accuracy (due to convergence problems)

C_ω	$A0$	$S0$	$A1$	$S1$
0	**111.54**	111.64	127.9	148.1
300	117.2	**82.02**	118.7	
1000	125.7	**34.43**	120.8	114.8
		$-\mathscr{I}m\,\lambda$		
0	0	0	-16.4	15.4
300	0	0	280	
1000	0	0	964	949

however the value of N_α unchanged. It turned out that these models converged very badly as the truncation parameters N_r and N_l were increased. The values given in Table 4 are therefore unfortunately not all of the same accuracy. However, the results suggest that there is no reason to hope that the non-axisymmetric modes will be more easily excited for thin disks.

3.2. Models with Different Rotation Curves.

Now we consider models with different rotation curves, i.e. different values of r_0.

Table 5 Marginal dynamo numbers for the same model as in Table 2, but with a different rotation curve with $r_0 = 0.2$. The transition from rigid to differential rotation occurs for this profile closer to the center than in the previous models for which we have used $r_0 = 0.5$

C_ω	A0	S0	A1	S1
−1000	**591**	1951	2512	2449
−300	**1012**	1775	1934	1850
−100	**1236**	1550	1696	1557
0	**1386**	1412	1420	1436
100	1595	**1283**	1556	1635
300	1798	**1076**	1851	2048
1000	1948	**657**	2457	2549
		$-\mathcal{Im}\,\lambda$		
−1000	0	±59.3	−670	−677
−300	0	0	−177	−173
−100	0	0	−35.6	−46.3
0	0	0	−0.57	+0.57
100	0	0	46.5	46.4
300	±6.23	0	172	133
1000	±59.2	0	677	260

Many galaxies are observed to make the transition from rigid to differential rotation quite close to their centers. In Table 5 we give the results for a model with $r_0 = 0.2$ instead of $r_0 = 0.5$ as in the previous case. There is now an even larger gap between the marginal dynamo numbers for axisymmetric and non-axisymmetric modes in the presence of differential rotation. Comparing the values of C_α for the S0- and S1-modes between $C_\omega = 0$ and $C_\omega = 1000$, we notice that the difference is, in the latter case, larger by a factor of two. According to the interpretation of Rädler (1986b), the field lines of non-axisymmetric fields are wound up by the influence of differential rotation leading so to an enhanced dissipation. Whilst the core region is nearly free of differential rotation we have an enhanced dissipation of non-axisymmetric modes for $r > r_0$. In the last case with $r_0 = 0.2$ almost the whole domain is affected. A close inspection of the rotation profile of Figure 2 shows that the maximum of $\partial\Omega/\partial r$ is for $r_0 = 0.2$ about three times larger than for $r_0 = 0.5$. We see that the differential rotation is obviously also here the reason for the large marginal dynamo numbers of non-axisymmetric modes. Values of C_α for $r_0 = 1.0$ are given in Table 6.

The field geometry of non-axisymmetric fields is hard to visualize (for a discussion see Krasheninnikova et al., 1990). One possibility is to adopt the vector potential $\mathbf{A} = \nabla \times (\hat{r}S) + \hat{r}T$. In a given plane we can plot contours of that component of $\mathbf{A}$, which is perpendicular to this plane. The contour lines correspond then to field lines of that part of the field which lies in this plane and is divergence-free. In Figure 4 we have plotted contours of A_θ in the equatorial plane for models with different values of r_0 and $C_\omega = 1000$. For $r_0 = 0.2$ there is a

Table 6 Marginal dynamo numbers for the same model as in Table 2, but the transition from rigid to differential rotation ocurs for this profile at $r_0 = 1.0$, i.e. at the boundary between the conducting halo and the vacuum exterior

C_ω	A0	S0	A1	S1
-1000	**244**	1657	1762	1690
-300	**633**	1853	1614	1538
-100	**10525**	1591	1466	1492
0	**1386**	1412	1420	1436
100	1603	**1110**	1492	1444
300	1854	**723**	1584	1613
1000	1654	**294**	1692	1761
		$-\mathcal{I}m\,\lambda$		
-1000	0	± 93.7	-982	-981
-300	0	0	-287	-288
-100	0	0	-0.57	$+0.57$
100	0	0	93.0	91.8
3000	± 2.7	0	288	287
1000	± 93.7	0	981	982

typical spiral field structure in the outer parts in the sphere. In contrast, for $r_0 > 0.5$ the field is concentrated close to the center. The reason for this behavior is understandable again from Figure 2: the field is located in that region of the sphere where the minimum of $|\partial\Omega/\partial r|$ occurs. Hence the magnetic field, which is generated in the region close to the center, is screened by the differential rotation. This effect was already anticipated by Krause (1983) for A-type stars with dynamo excitation in their convective cores.

A particular property of the rotation curves used here is that $|\partial\Omega/\partial r|$ never vanishes. This is in contrast to the profiles used by Steenbeck and Krause (1969), for which Krause (1971) and Roberts and Stix (1972) found a preference of the $S1$-mode for certain values of C_ω. From Figure 2 we see that regions with small $|\partial\Omega/\partial r|$ are not only possible for large values of r_0, but also when r_0 is very small. It may be that the value $r_0 = 0.2$, adopted for the model of Table 5, is still too large. We have therefore included in Table 7 also some results for $r_0 = 0.1$. Comparing this with the case $r_0 = 0.2$ we find that the marginal dynamo numbers of the axisymmetric modes now increase drastically, whereas those of the non-axisymmetric fields decrease only slightly. This is shown more clearly in Figure 5, where we have summarized the variation of the marginal dynamo numbers for different values of the rotation parameters r_0. It might be desirable to take the calculation to still smaller values of r_0. However, a higher computational accuracy would then also be needed.

Another visualization of non-axisymmetric fields is given directly by contour plots of certain field components. In Figure 6 we have plotted contours of B_ϕ in an arbitrary meridional plane for the same models as in Figure 4. A negative value of B_ϕ is indicated by a dotted line. Note the rapidly alternating sign of B_ϕ for
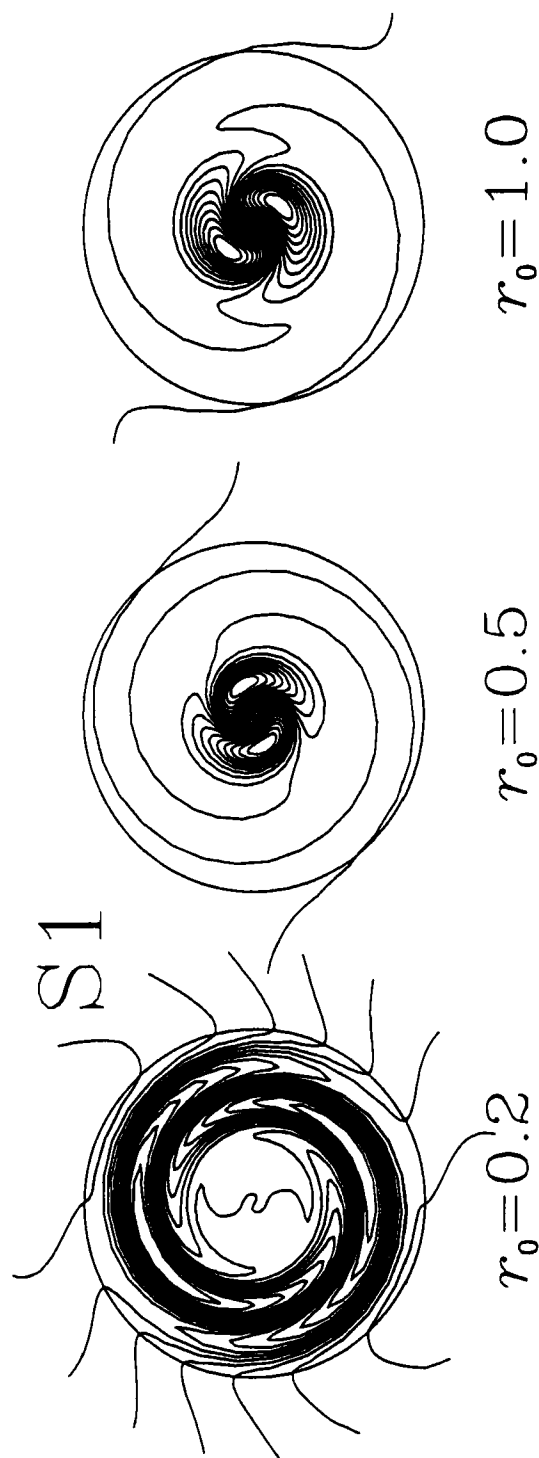
Figure 4 Contours of constant A_θ in the equatorial plane for the $S1$-mode for different values of r_0. $C_\omega = 1000$. Note the field concentration toward the center for $r_0 = 0.5$ and $r_0 = 1$.

Table 7 Marginal dynamo numbers for the same model as in Table 2 and in Table 5, but the transition from rigid to differential rotation occurs at $r_0 = 0.1$, i.e. still closer to the center than in the model of Table 5

C_ω	A0	S0	A1	S1
0	**1386**	1412	1420	1436
100	1448	**1366**	1482	1525
300	1586	**1280**	1779	1789
1000	1841	**1043**	2364	2240

		$\mathscr{I}m\,\lambda$		
0	0	0	−0.57	+0.57
100	0	0	23.0	24.1
300	±1.7	0	90.8	54.1
1000	±9.3	0	152	146
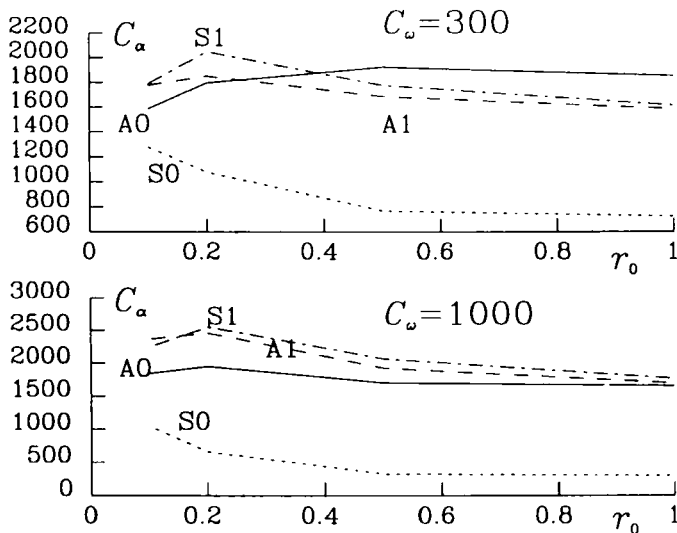
Figure 5 The variation of the marginal dynamo numbers for different values of r_0 for $C_\omega = 300$ and $C_\omega = 1000$. Note that the marginal dynamo numbers of the axisymmetric modes increase drastically towards smaller values of r_0, whereas those of the non-axisymmetric fields decrease slightly.

$r_0 = 0.2$ in the outer parts of the sphere and close to the equator. For $r_0 > 0.5$ the sign of B_ϕ is, at least within the equatorial plane, more or less the same.

The most preferred magnetic field mode was, in the three models considered above, of S0-type. The contours of constant B_ϕ for this S0-field are shown in Figure 7 in a meridional plane. It was stressed by Krause and Meinel (1988) that
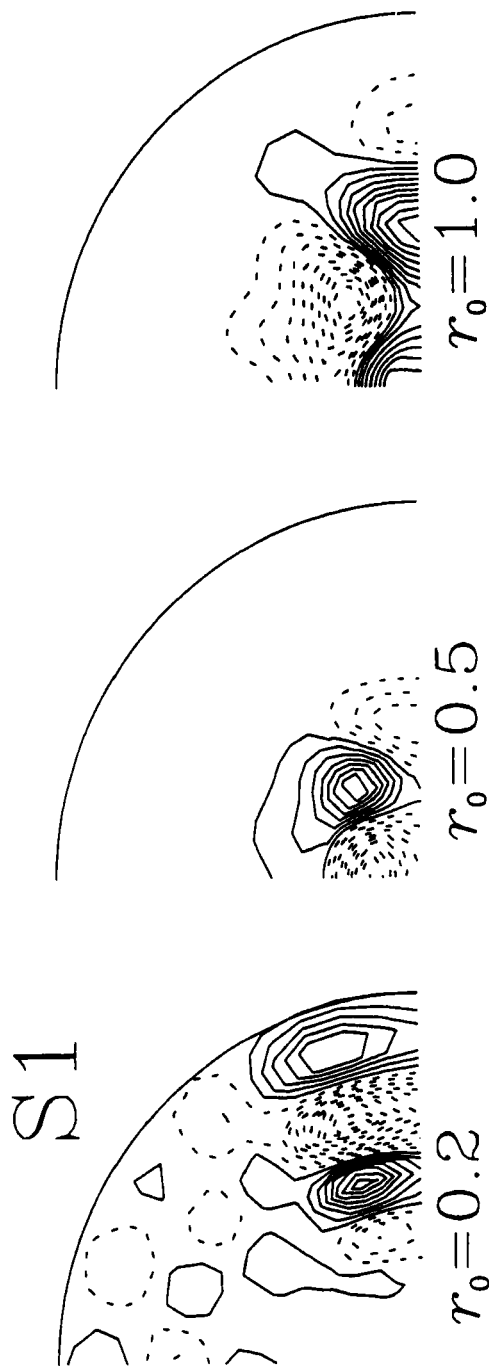
Figure 6 Contours of constant B_ϕ in an arbitrary meridional plane for the same models as in Figure 4. Dotted contours refer to a negative value. Note the rapidly alternating sign for $r_0 = 0.2$ in the outer parts.
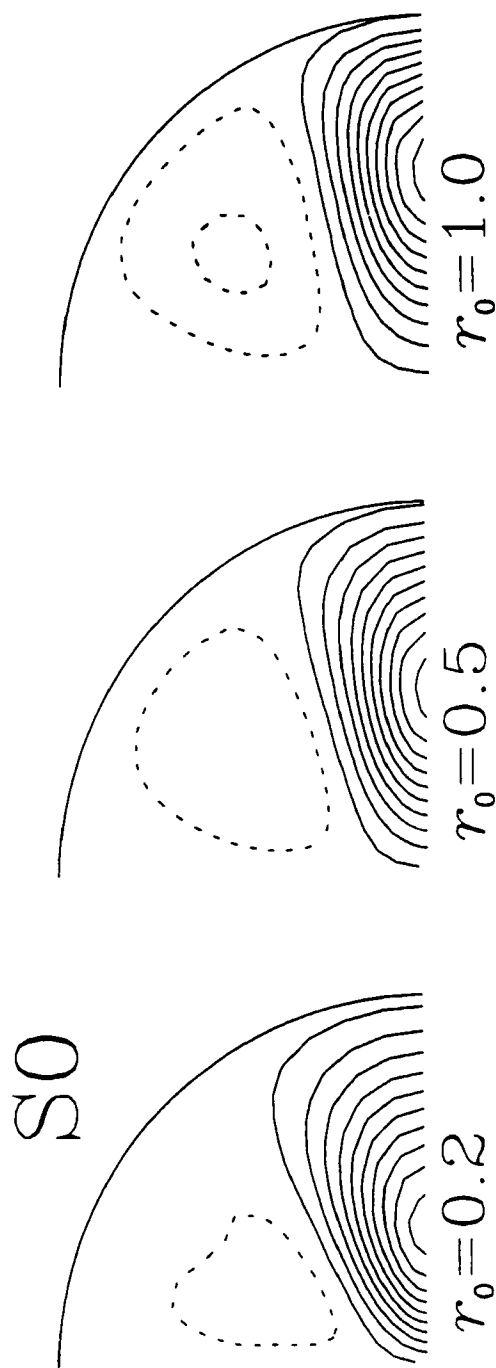
Figure 7 Contours of constant B_ϕ in a meridional plane for the same models as in Figure 6, but for the S0-mode. Note a stronger concentration toward the equatorial plane for increasing r_0.

only the solution with the smallest marginal dynamo number—here the $S0$-type solution—is stable and physically relevant. On the other hand, further into the nonlinear regime other solutions (e.g. 'mixed solutions') can also occur (see Brandenburg et al., 1989a). This was shown also for galactic nonlinear $\alpha\omega$-dynamos by Moss and Tuominen (1990). They found long-term oscillations between $A0$- and $S0$-symmetry in axisymmetric models. Since $A1$- and $S1$-modes are located between the $S0$- and $A0$-modes (for $r_0 > 0.4$ and $C_\omega = 300$, see Figure 5), we would expect that non-axisymmetric contributions may be involved in these oscillations.

Because of that possibility we have also studied here the $S1$-mode, which is much harder to excite, in more detail. In Figure 8 we demonstrate the effect of increasing differential rotation on the field geometry of the $S1$-mode. The differential rotation is varied from $C_\omega = 100$ to $C_\omega = 1000$. The phenomenon of field lines being wound up is best seen in the last case with $C_\omega = 1000$. Note that in the case of weak differential rotation the field seems still to be concentrated close to the center. Only when C_ω exceeds a value of about 500 does flux expulsion towards the outer regions occur. Already from this geometrical appearance one might suggest that, if bisymmetric galactic fields are really caused by an axisymmetric $\alpha\omega$-effect, the magnetic Reynolds number for the differential rotation, C_ω, must be of the order of 10^3. This is, however, in contradiction with the fact that the effective dissipation of non-axisymmetric fields is, under such conditions, much higher than for axisymmetric fields. This suggests that the bisymmetric fields observed in some galaxies are caused by other important properties, for example by an anisotropic or non-axisymmetric α-effect.

4. CONCLUSIONS

The results presented here are a first attempt to investigate systematically the excitation conditions of simple mean-field dynamos with flat α-effect distribution avoiding local approximations. The results for different degrees of flatness and various rotation curves seems to exclude the possibility of a preferred non-axisymmetric mode under the assumption of an isotropic and axisymmetric α-effect. We suggest therefore that one of these restrictions should be relaxed. The spherical models by Rüdiger (1980) for a non-isotropic α-effect (i.e. $\mathscr{E} \sim \hat{z}B_z$) show a very strong preference for non-axisymmetric modes, which may remain also for flat α-effect distributions in the presence of differential rotation. This type of anisotropy is much better suited for a treatment in cylindrical coordinates (Elstner et al. 1990).

The dependence of the marginal dynamo numbers on the thickness of the disk and on the shape of the rotation curve does not seem to change the gross behavior very much. In most of the cases investigated here a stationary $S0$-mode is preferred, which is in agreement with the models by Stix (1975). We have demonstrated that this result is connected with the flat geometry and that an oscillatory $A0$-mode, similar to the Steenbeck–Krause (1969) models, is recovered in the non-flat case ($z_0 = 1$).

The rotation curves in galaxies have the property that $|\partial\Omega/\partial r|$ is always different from zero, i.e. winding-up of field lines does occur throughout the entire domain.
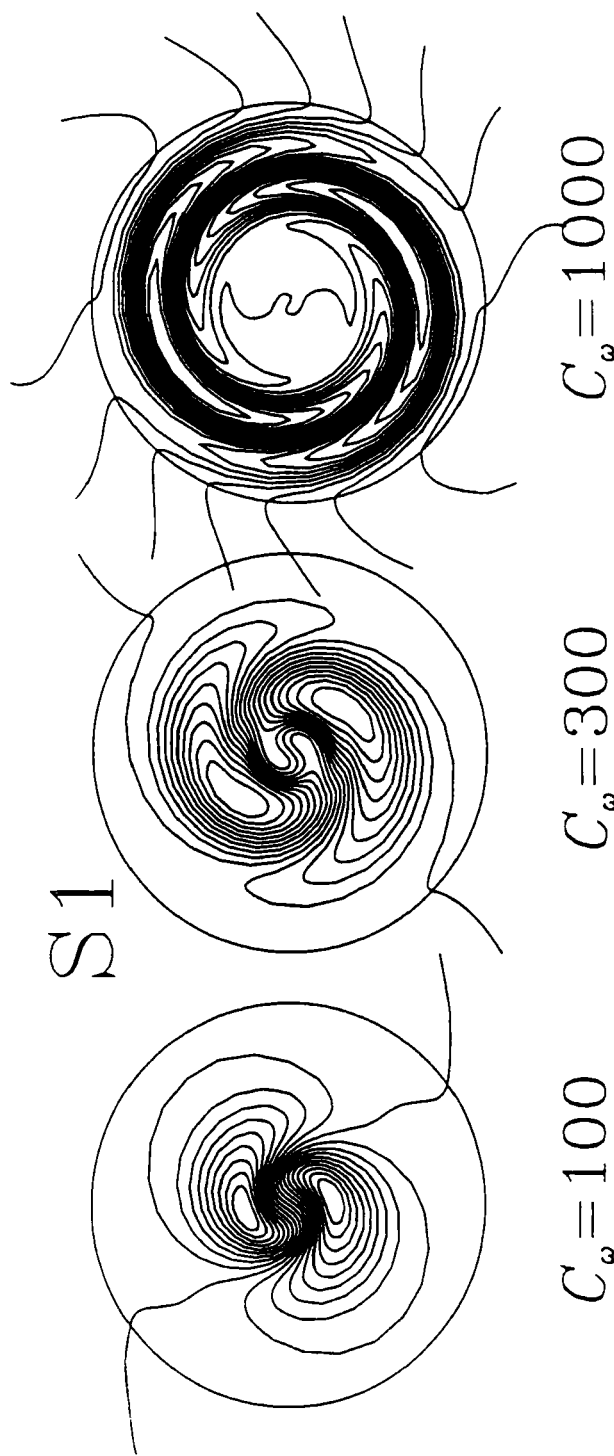
Figure 8 The effect of differential rotation on the field geometry of the non-axisymmetric modes (S1) demonstrated with contours of constant A_θ in the equatorial plane. The differential rotation is varied from $C_\omega = 100$ to $C_\omega = 1000$.

This is one of the reasons why non-axisymmetric modes are hard to excite. Earlier results showing a preference of non-axisymmetric modes in spherical models in the presence of weak differential rotation are based on rotation curves for which $|\partial\Omega/\partial r|$ vanishes in most parts of the sphere. This finding therefore does not apply to galaxies. Another important difference is the degree of overlap between the α- and ω-effect induction layers. In the case of an overlap, a weak differential rotation can already decrease the marginal dynamo number of axisymmetric fields substantially and so make non-axisymmetric fields comparably harder to excite. The opposite is the case for models with a gap between the two induction layers. At present there is, however, no observational evidence for such a gap in galaxies. Finally, we want to mention that models with other rotation curves should be investigated too, in particular for the case of smaller values of r_0 than was possible in the present study.

References

Baryshnikova, Y., Ruzmaikin, A. A., Sokoloff, D. D. and Shukurov, A., "Generation of large-scale magnetic fields in spiral galaxies," *Astron. Astrophys.* **177**, 27 (1987).

Brandenburg, A., Krause, F., Meinel, R., Moss, D. and Tuominen, I., "The stability of nonlinear dynamos and the limited role of kinematic growth rates," *Astron. Astrophys.* **213**, 411 (1989a).

Brandenburg, A., Rädler, K.-H., and Tuominen, I., "On the generation of non-axisymmetric magnetic fields in mean-field dynamos," *Geophys. Astrophys. Fluid Dyn.* in press (1989b).

Donner, K. J. and Brandenburg, A., "Magnetic field structure in differentially rotating discs," *Geophys. Astrophys. Fluid Dyn.*, this meeting (1990).

Elstner, D., Meinel, R. and Rüdiger, G., "Galactic dynamo models without sharp boundaries," *Geophys. Astrophys. Fluid Dyn.*, this meeting (1990).

Krasheninnikova, Yu. S., Ruzmaikin, A. A., Sokoloff, D. D. and Shukurov, A. M., "Galactic dynamo in a thin disk: axisymmetric and non-axisymmetric modes," *Geophys. Astrophys. Fluid Dyn.*, this meeting (1990).

Krause, F., "Zur Dynamotheorie magnetischer Sterne: Der 'symmetrische Rotator' als Alternative zum 'schiefen Rotator'," *Astron. Nachr.* **293**, 187 (1971).

Krause, F., "On the nature of magnetic stars," In: *Stellar and Planetary Magnetism*, (Ed. A. M. Soward) Gordon and Breach Science Publishers, New York-London-Paris, p. 205 (1983).

Krause, F., "How well is dynamo theory of flat objects developed?," *Geophys. Astrophys. Fluid Dyn.*, this meeting. (1990).

Krause , F. and Meinel, R., "Stability of simple nonlinear α^2-dynamos," *Geophys. Astrophys. Fluid Dyn.* **43**, 95 (1988).

Krause, F. and Rädler, K.-H., *Mean-Field Hydrodynamics and Dynamo Theory*, Akademie-Verlag, Berlin and Pergamon Press, Oxford (1980).

Moss, D. and Tuominen, I., "Nonlinear galactic dynamos," *Geophys. Astrophys. Fluid Dyn.*, this meeting (1990).

Rädler, K.-H., "Investigations of spherical kinematic mean-field dynamo models," *Astron. Nachr.* **307**, 89 (1986a).

Rädler, K.-H., "On the effect of differential rotation on axisymmetric and non-axisymmetric magnetic fields of cosmical bodies," *Plasma Physics*, ESA **SP-251**, 569 (1986b).

Roberts, P. H. and Stix, M., "α-effect dynamos, by the Bullard–Gellman formalism," *Astron. Astrophys.* **18**, 453 (1972).

Rüdiger, G., "Rapidly rotating α^2-dynamo models," *Astron. Nachr.* **301**, 181 (1980).

Rüdiger, G., "On the α-effect in galaxies," *Geophys. Astrophys. Fluid Dyn.*, this meeting. (1990).

Ruzmaikin, A. A., Shukurov, A. M. and Sokoloff, D. D., *Magnetic Fields of Galaxies*, D. Reidel & Kluwer Publ. (1988).

Stix, M., "The galactic dynamo," *Astron. Astrophys.* **42**, 85 (1975).

Steenbeck, M. and Krause, F., "Zur Dynamotheorie stellarer und planetarer Magnetfelder, I. Berechnung sonnenähnlicher Wechselfeldgeneratoren," *Astron. Nachr.* **291**, 49 (1969).

Zeldovich, Ya. B., Ruzmaikin, A. A. and Sokoloff, D. D., *Magnetic Fields in Astrophysics*, Gordon and Breach, pp. 149–168 (1983).